Intersubunit Proximity of Residues in the RecA Protein As Shown by Engineered Disulfide Cross-Links†

Mark C. Skiba,‡ Karen M. Logan,‡ and Kendall L. Knight*

Department of Biochemistry and Molecular Biology, University of Massachusetts Medical School, 55 Lake Avenue North, Worcester, Massachusetts 01655-0103

Received May 17, 1999; Revised Manuscript Received July 9, 1999

ABSTRACT: Mutational studies of regions that make up the oligomeric interface within the RecA protein filament structure have shown that F217 is an important determinant of RecA function and oligomer stability. All substitutions, other than Tyr and Cys, completely inhibit RecA activities and exhibit a substantial decrease in protein filament stability [Skiba, M. C., and Knight, K. L. (1994) *J. Biol. Chem. 269*, 3823−3828; Logan, K. M., et al. (1997) *J. Mol. Biol. 266*, 306−316]. Although the RecA crystal structure exhibits no obvious constraints that explain this mutational stringency, the structure does reveal a hydrophobic pocket in the neighboring monomer that may accommodate the F217 side chain. Together with the F217C mutation, we have introduced a series of Cys substitutions within the interacting surface on the neighboring monomer and have tested for disulfide formation under various conditions, e.g., with or without ATP and ssDNA. We show that the location of F217 in the crystal structure is in general agreement with its position in the catalytically active RecA−ATP−DNA complex. Functional studies with the mutant proteins support the idea that ATP-induced movement of the wild-type F217 side chain toward this hydrophobic pocket is important in mediating allosteric changes in the RecA protein structure.

The bacterial RecA protein is a moderately sized 38 kDa protein, which upon interaction with ATP and single-stranded DNA, forms a helical nucleoprotein filament. This polymeric oligomer is the active form for both the catalysis of homologous genetic recombination and cleavage of the LexA repressor, two distinct catalytic activities carried out by RecA in its role as the central enzymatic and regulatory component in a complex system of functions which promote cell survival following DNA damage (*1*−*5*).

In an effort to identify important determinants of the oligomeric structure of RecA, we previously introduced a number of mutations into one area of the protein (*6*) which is seen in the crystal structure (*7*) to contain a variety of intersubunit contacts. The sequence spanning residues 213−222 contains five amino acids (N213, K216, F217, Y218, and R222) whose side chains extend across the interface and contact positions in the neighboring subunit (*6*, *7*). Of these five positions, we found that three are far more sensitive to substitution (F217 > K216 > R222) than the other two (N213 and Y218) with regard to inhibition of recombinational DNA repair and homologous recombination activities (*6*), and effects on coprotease function (M. C. Skiba and K. L. Knight, unpublished results). Of 15 substitutions at position 217, F217Y maintains wild-type-like recombination activities in vivo, F217C maintains approximately 20% of the recombination activities, and the 13 other substitutions, which include a variety of polar and nonpolar amino acids, result in complete inactivation of all RecA functions (ref *6*, this study, and unpublished results of M. C. Skiba, K. M. Logan, S. Eldin, and K. L. Knight). We also studied the effects of mutations at these residues on the oligomeric structure of RecA. Unlike wild-type RecA, all substitutions analyzed at K216 and R222 inhibited formation of stable protein filaments in the absence of DNA. The F217Y and F217C mutations still permitted filament formation, although the stability was somewhat reduced (*8*; K. M. Logan and K. L. Knight, unpublished results).

While the mutational stringency at K216 and R222 can be rationalized in terms of the contacts observed in the crystal structure, there appear to be no structural constraints that explain the stringency at F217 (*6*). However, several hydrophobic residues are seen clustered within a pocket in the neighboring subunit and may serve to stabilize a cross-subunit interaction with F217. In addition, the helical pitch of the RecA filament in the crystal structure is midway between that observed for the inactive ADP-bound form (≈70 Å) and the active ATP-bound form (≈95 Å), and therefore raises some question about whether the positions of certain residues in the crystal structure correctly predict their position in the catalytically active RecA−ATP−DNA complex (*9*). Experiments in this study have been designed to test the cross-subunit proximity of position 217 to residues in the neighboring monomer. We find that the position of F217 in the RecA crystal structure is in general agreement with its position in the catalytically active form of the enzyme. In addition, our data suggest that movement of the F217 side chain during the catalytic cycle of ATP binding and hydrolysis is important to the allosteric nature of RecA function.

† Supported by NIH Grant GM44772 to K.L.K.

* Corresponding author. Phone: (508) 856-2405. Fax: (508) 856-6231. E-mail: kendall.knight@umassmed.edu.

‡ These authors contributed equally to this project.

10.1021/bi991118z CCC: $18.00
Published on Web 08/25/1999

MATERIALS AND METHODS

Materials. LB broth and LB medium were prepared as described previously (*10*) and contained 100 μg/mL ampicillin. MacConkey-lactose plates were prepared according to the manufacturer's instructions (Difco) and contained 0.5% lactose and 100 μg/mL ampicillin. Stock solutions of DTNB[1] (35 mM) and NEM (0.3 M) were made fresh in 200 mM K_2HPO_4/KH_2PO_4 (pH 8.0) and 1 M Tris-HCl (pH 8.2), respectively. The 90-base oligonucleotide used for the gel shift ssDNA binding assays and all mutagenic oligonucleotides were made using an Applied Biosystems 392 DNA/RNA synthesizer. [γ-^{32}P]dATP was from New England Nuclear. dATP, ATP, and ADP were from Sigma. NaF and $Al(NO_3)_3$ were from J. T. Baker.

Strains and Plasmids. Wild-type and mutant *recA* genes in this study are carried in either of two plasmids, pTRecA230 or pTRecA520, both of which have *recA* under control of the inducible *tac* promoter, and both of which are derived from pTRecA103 (*11*). *Escherichia coli* strains MV1190 (*11*) and DE1663′ (*12*) were used for all in vivo screens for RecA function and for purification of wild-type and all mutant RecA proteins.

Mutagenesis. Amino acid substitutions were introduced using either a variation of a previously described cassette mutagenesis procedure (*6*) or a PCR-based method (QuikChange, Stratagene). Substitutions were identified by DNA sequence analysis.

Mini-Lysate Procedure. Overnight cultures were diluted 1:100 in LB-amp medium (4 mL) and incubated for approximately 3 h at 37 °C. IPTG (final concentration of 3 mM) was added to one-half of each culture and incubation continued for 3.0 h. Cells were harvested, suspended in 200 μL of Laemmli sample buffer, heated at 100 °C for 2 min, and centrifuged for 15 min. The pellet was discarded, and 5 μL of the supernatant was loaded onto a 10% SDS−polyacrylamide gel. Gels were analyzed using a FluorS MultiImager (Bio-Rad).

In Vivo Activities of recA Mutants. Assays for recombinational DNA repair involved measurements of cell survival following exposure to UV light or mitomycin C and were performed as previously described (*12*). Cell growth across a series of time zones of exposure was ranked from 0 to 4, and fractional survival at 30 s was calculated from the slope of a line resulting from a plot of the relative rate of growth versus time. The extent of RecA-mediated cleavage of the LexA protein was measured using MacConkey-lactose plates as previously described (*12*).

Determination of the Oligomeric Properties of Mutant RecA Proteins. The effect of mutations on the oligomeric properties of RecA was determined by analyzing the elution profile of each protein on a Superose 6 HR gel filtration column as previously described (*8*). The concentration of RecA protein in the column load was always $\geq$26 μM.

Protein Purification. Purification of wild-type and mutant RecA proteins was performed using several variations of a previously described procedure (*13*). For mutant proteins, the concentration of βME was increased in all buffers from 5 to 20 mM to prevent spontaneous disulfide bond formation. Although the details of the purification protocols for each mutant protein were slightly different, purification of each was achieved using a combination of chromatography steps which included (i) single-stranded DNA cellulose, (ii) ceramic hydroxyapatite, (iii) ATP−agarose, and (iv) Sephacryl S-1000. Details of the purifications are available on request.

DNA Binding. Reactions (volume of 30 μL) were performed in buffer containing 10 mM Na_2HPO_4, NaH_2PO_4 (pH 7.4), 138 mM NaCl, 27 mM KCl, and 15 mM $MgCl_2$, and included 10 μM 5′-end labeled oligonucleotide (90 bases) and 0.5 mM ATPγS where indicated. Protein concentrations varied from 0.5 to 5.0 μM. Reactions were initiated with the addition of labeled oligonucleotide, and mixtures were incubated for 45 min at 37 °C followed by addition of glycerol to a final concentration of 20% (w/v). Reaction mixtures were loaded onto a nondenaturing 8% polyacrylamide gel and electrophoresed in $^1/_2\times$ TBE buffer (*10*). Gels were dried and analyzed using a Personal Molecular Imager FX and QuantityOne software (Bio-Rad).

ATPase Activity. Single-stranded DNA-dependent hydrolysis of ATP was assessed using a PEI chromatography method as previously described (*13*, *14*).

LexA Cleavage. RecA-mediated cleavage of the LexA repressor was assessed as previously described (*13*). Briefly, reaction mixtures (40 μL) contained 1 μM wild-type or mutant RecA protein, 1 mM ATPγS, and 35 μM M13 single-stranded DNA. Reactions were started with the addition of LexA protein to a final concentration of 6 μM. Samples (8 μL) were removed at various time points from 0 to 60 min, added to Laemmli sample buffer (10 μL), heated to 95 °C, and loaded onto 15% SDS−polyacrylamide gels. Gels were stained with Coomassie blue (R250), and the percentage of LexA cleavage was determined by analyzing both the decrease in the amount of intact LexA protein and the increase in the amount of cleavage products using a FluorS MultiImager (Bio-Rad).

Intersubunit Disulfide Cross-Links. Formation and analysis of intersubunit disulfide cross-links was performed using the following procedure. Protein (50 μg) was prereduced in the presence of 20 mM βME (20 min at 22 °C) and desalted into reaction buffer [100 mM Tris-HCl (pH 8.5), 0.1 mM EDTA, 30 mM NaCl, 15 mM $MgCl_2$, and 5% glycerol] using a Microcon concentrator (Amicon). Disulfide cross-links were induced by mixing DTNB (final concentration of 20 mM) with protein (final concentration of 30 μM) and incubating for 60 min at 37 °C. NEM was added to a final concentration of 30 mM, followed immediately by addition of SDS to a final concentration of 1.0%. The reaction mixture was incubated for 10 min at 22 °C; Laemmli loading dye (without βME) was added, and samples were electrophoresed on 8% SDS−polyacrylamide gels. Control experiments included (i) reactions performed in the absence of DTNB to observe potential spontaneous disulfide formation and (ii) incubation with βME (final concentration of 150 mM) following cross-linking to ensure that all higher-molecular mass protein forms observed on gels contained reducible disulfides. Gels were stained with Coomassie blue (R250), or Western blots were performed using polyclonal rabbit anti-RecA antibodies as previously described (*11*). Gels and blots were analyzed using a FluorS MultiImager (Bio-Rad).

[1] Abbreviations: ss, single-stranded; βME, β-mercaptoethanol; IPTG, isopropyl 1-thio-β-D-galactopyranoside; ATPγS, adenosine 5′-*O*-(thiotriphosphate); PEI, polyethylenimine; DTNB, 5,5′-dithiobis(2-nitrobenzoic acid); NEM, *N*-ethylmaleimide.

Mixtures whose reactions were carried out in the presence of nucleotide cofactors contained one the following: 1.0 mM dATP, 1.0 mM ATP, 0.5 mM ATPγS, or ADP−AlF_4. ADP−AlF_4 was prepared by mixing 1.0 mM ADP, 10 mM NaF, and 0.4 mM $Al(NO_3)_3$ (*15*). When present, single-stranded M13 DNA was added to a final concentration of 70 μM (nucleotides).

Control experiments showed that the three Cys residues in wild-type RecA did not interfere with our analyses of the cross-linking efficiency of the cross-subunit Cys mutations (see Results). Therefore, although it has been shown that none of these Cys residues is essential for RecA function (*16*), we did not mutate the native Cys residues so that the functional and structural integrity of the protein was not further compromised.

RESULTS

Design of Cys Mutations. In Figure 1, we show a view of the area surrounding F217 as seen in the RecA crystal structure (*7*). The space filling model in panel A shows that the F217 side chain (red) packs close to the side chains of T121, T150, and I155 (green) in the neighboring monomer. A more detailed view (Figure 1, panels B and C) shows the arrangement of side chains in this region and the cross-subunit distance between the β-carbons for T121−F217 (6.78 Å), T150−F217 (6.62 Å), and I155−F217 (5.42 Å). As a direct test of the cross-subunit proximity of residues in this region, we created a number of double Cys mutations to check the efficiency with which they formed disulfide bonds. Each double mutant carried a Cys substitution at F217 and another at one of nine positions on the opposite side of the subunit interface: I93, A95, D120, T121, A125, S145, A148, T150, or I155. The distances between the β-carbon of F217 and each of these side chains are given in Table 1. Proteins that could be stably overproduced were purified to homogeneity and tested for their ability to form disulfide bonds under a variety of conditions.

Effects of Designed Cys Mutations on Protein Stability. As a first step in characterizing the effects of Cys substitutions on protein stability, we performed a mini-lysate procedure following induction of the p_{tac}-*recA* plasmid-borne genes with IPTG. Analysis of the protein content in crude cell lysates with Coomassie-stained SDS gels showed that the C120 mutant produced no protein, whereas the C145 and C148 single mutant proteins were present at approximately 30% of the level of wild-type RecA. The corresponding double mutants (C145/217 and C148/217) showed no band corresponding to RecA protein (data not shown). Western blot analysis of crude cell extracts confirmed the absence of RecA protein for these double-Cys mutants (data not shown). All other single-Cys (C93, C95, C121, C125, C150, C155, and C217) and double-Cys mutants (C93/217, C95/217, C121/217, C125/217, C150/217, and C155/217) exhibited normal levels of IPTG-inducible RecA protein.

Effects of Cys Mutations on RecA Oligomeric Properties. The ability of mutant proteins to form wild-type-like oligomeric filaments was assessed using a gel filtration assay (*8*). The concentration of RecA protein that was loaded onto the column (≈30 μM monomer) is equivalent to that used in the cross-linking experiments. A Superose 6 profile of wild-type RecA shows that in the absence of ATPγS, the majority of protein elutes between the column void (8 mL) and 11 mL (Figure 2A). This corresponds to oligomers with average

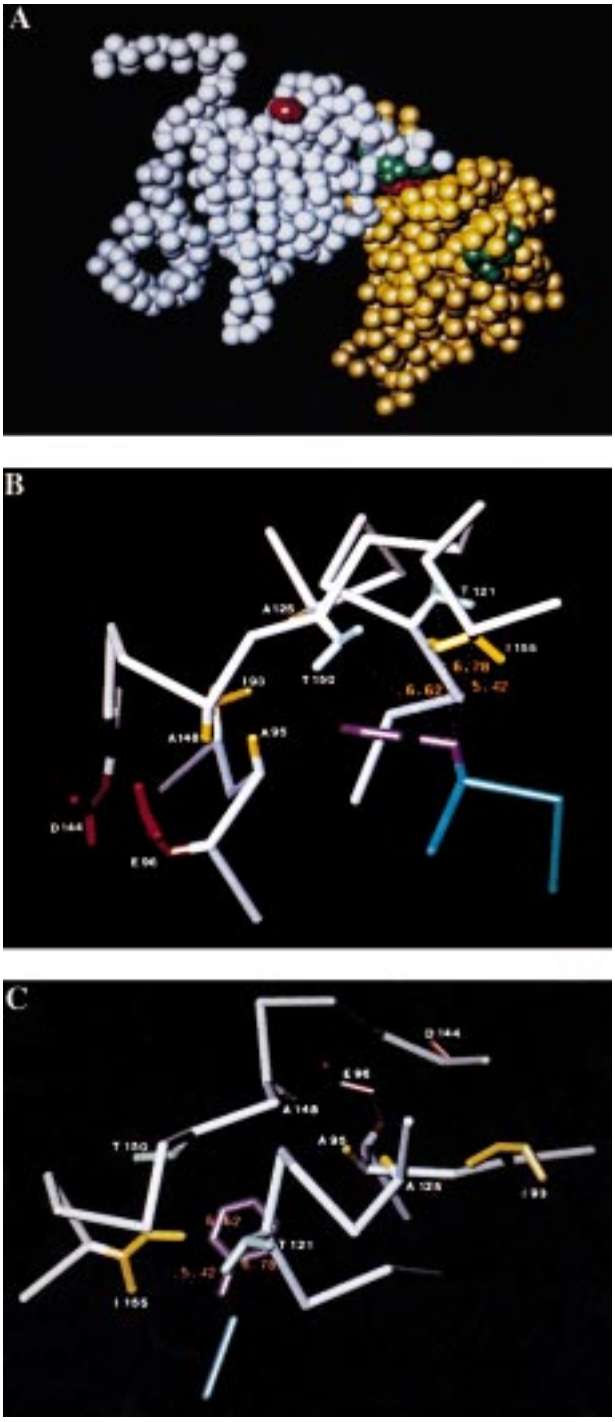

FIGURE 1: Region of the RecA subunit interface surrounding F217. (A) An α-carbon structure of a RecA dimer, taken from the crystal structure of the helical RecA polymer (*7*). α-Carbons are yellow and white in the neighboring monomers. Close packing of the F217 side chain (red) in one monomer with T121, T150, and I155 (green) in the neighboring monomer can be seen. (B) Detailed view of the proximity of the F217 side chain from one monomer to positions within the neighboring monomer. The F217 side chain is violet. Hydrophobic residues that make up the pocket are I93, A95, A125, and A148 (yellow). Other highlighted residues in the neighboring monomer include T121 and T150 (light blue), I155 (yellow), and E96 and D144 (red). E96 and D144 are ATP site catalytic residues (see the text). Dotted lines represent distances between the Cβ of F217 and the Cβ of T121 (6.78 Å), T150 (6.62 Å), and I155 (5.42 Å). (C) Top view of the image in panel B.

Table 1: $C\beta_1-C\beta_2$ Distances between Phe217 and Residues in the Neighboring Subunit

side chain	distance from Phe217 Cβ (Å)	side chain	distance from Phe217 Cβ (Å)
Ile93	13.63	Ser145	14.12
Ala95	8.32	Ala148	9.54
Asp120	5.62	Thr150	6.62
Thr121	6.78	Ile155	5.42
Ala125	10.51		

molecular masses ranging from $\geq 5 \times 10^6$ to 1×10^6 Da. In the presence of ATPγS, the oligomeric distribution shows a characteristic shift to lower-molecular mass species (Figure 2A), consistent with previous electron microscopic, light scattering, and gel filtration studies (*8*, *17*−*19*). Superose 6 profiles of three mutant proteins, C217, C121/217, and C155/217, show that each also forms high-molecular mass oligomers with variable amounts of lower-molecular mass species (Figure 2B−D). Therefore, Cys substitutions at these positions do not significantly compromise the oligomeric properties of the mutant proteins. However, in contrast to wild-type RecA, the ATP-induced decrease in oligomer size is not observed. The loss of this effect correlates with the F217C mutation. All mutants which have this substitution (C93/217, C95/217, C125/217, and C150/217) exhibit similar behaviors, while those which do not have the F217C substitution (C93, C95, C121, C125, C150, and C155) maintain the ATP-induced decrease in oligomer size (data not shown). The lack of this effect for all mutant proteins with the F217C substitution is not due to a simple defect in

Table 2: In Vivo DNA Repair and LexA Coprotease Activities[a]

Cys mutant	fraction UV survival/30 s	coprotease
93	1.00	i
95	0.15	−
121	1.00	i
125	0.90	i
150	1.00	c
155	1.00	c
217	0.25	c
93/217	0.25	c−
95/217	0.10	−
121/217	0.25	c
125/217	0.15	−
150/217	0.25	c
155/217	0.38	c
pTRecA230	1.00	i
pZ150	0.00	−

[a] i means inducible (increase in activity following DNA damage). c means constitutive activity (activity in the absence of DNA damage which is similar to activity in the presence of damage). c− is like c, but significantly less activity in both the absence and presence of DNA damage. − means undetectable.

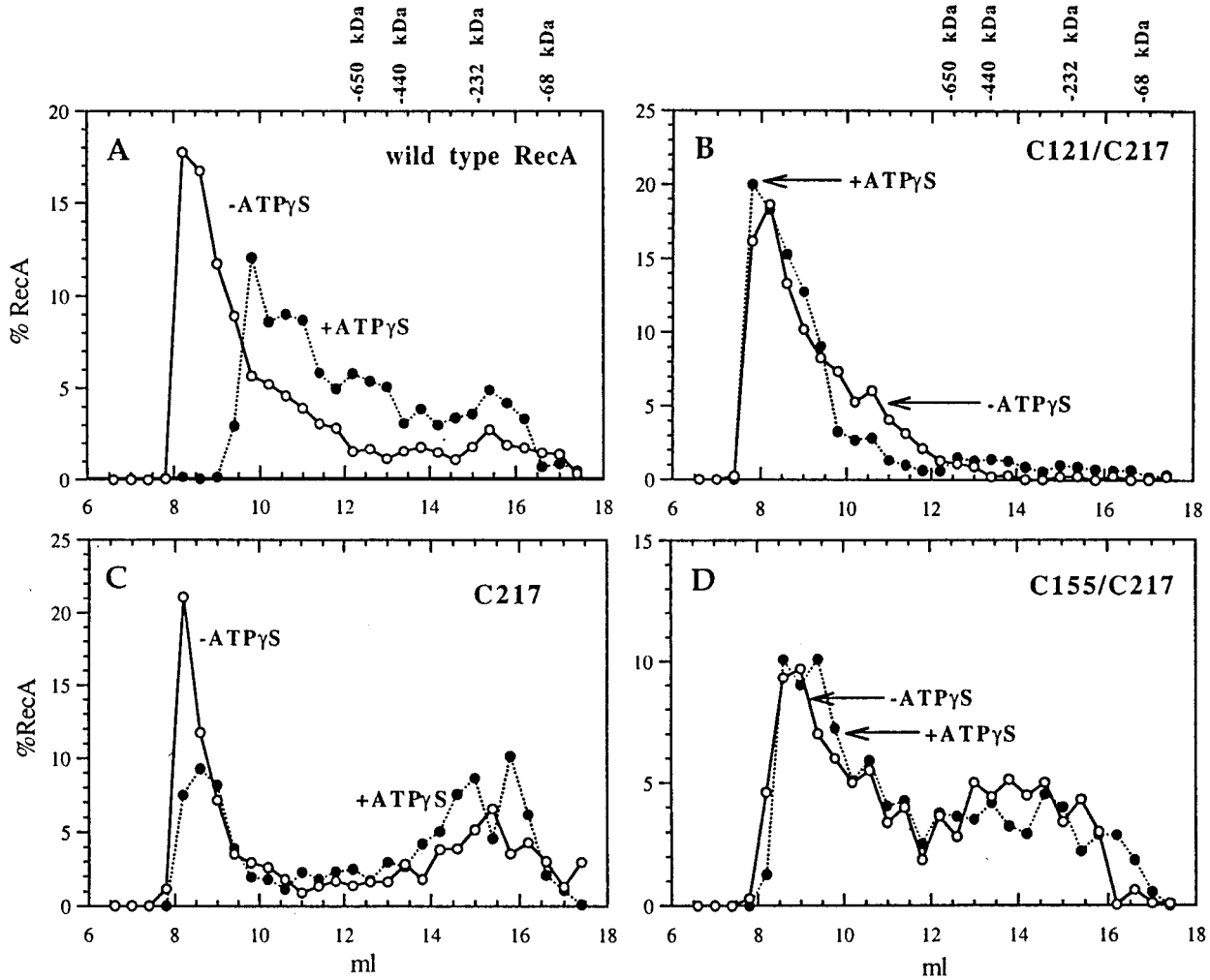

FIGURE 2: Gel filtration profiles showing the formation of high-molecular mass oligomers of wild-type RecA and three mutant proteins. Superose 6 gel filtration assays were performed as described in the text. Mutant proteins C121/217 (B), C217 (C), and C155/217 (D) form high-molecular mass oligomers, but no longer undergo the ATP-induced shift in oligomeric distribution as seen with wild-type RecA (see the text). Molecular mass markers are thyroglobulin (650 kDa), ferritin (440 kDa), catalase (232 kDa), and BSA (68 kDa).

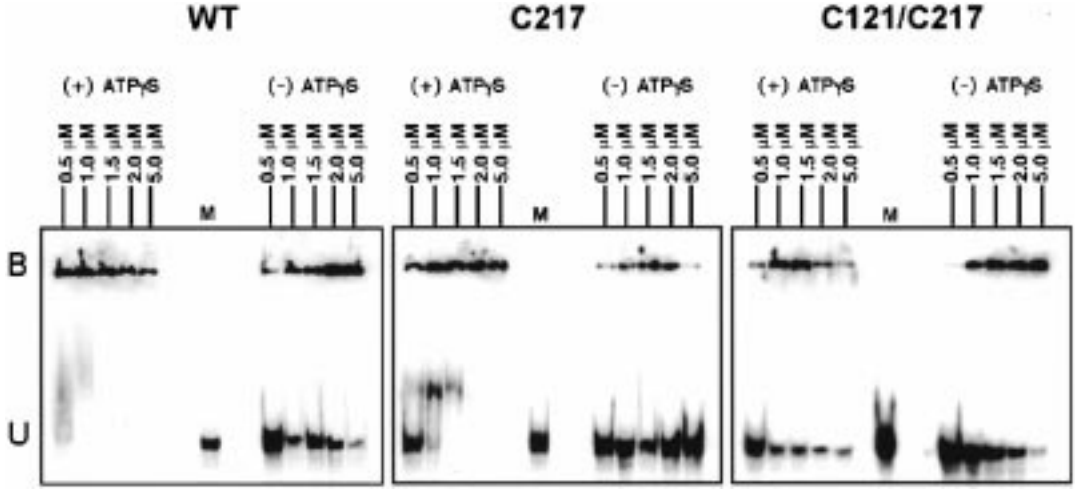

FIGURE 3: Gel shift ssDNA binding assays. Protein was incubated with a 5′-end-labeled oligonucleotide, in either the presence or absence of 0.5 mM ATPγS, and complexes were analyzed on 8% nondenaturing acrylamide gels. Protein concentrations in the reaction mixes varied from 0.5 to 5.0 μM. U denotes unbound radiolabeled oligonucleotide, B protein−oligonucleotide complexes in the gel well, and M marker (unreacted radiolabeled oligonucleotide).

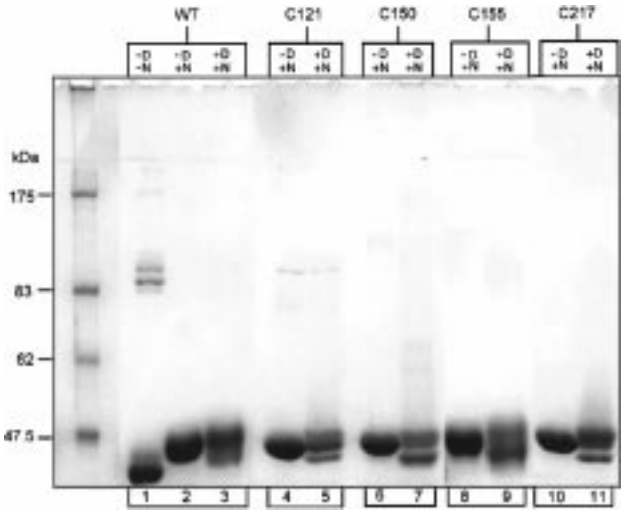

FIGURE 4: Disulfide cross-linking performed using wild-type RecA and the single-Cys mutant proteins C121, C150, C155, and C217. Reaction mixtures contained 30 μM protein, and reactions were performed in the absence (−D) or presence (+D) of DTNB, followed by incubation with NEM (+N) as described in Materials and Methods. In the absence of NEM (−N; lane 1), a small amount of random disulfide bonds forms with the addition of SDS just prior to gel electrophoresis. Molecular mass markers are shown on the left.

ATP binding because each protein carries out functions that require ATP binding (see below).

In Vivo RecA Functions. Two in vivo functions that require the formation of active RecA−DNA filaments are recombinational DNA repair and coprotease activity. The results shown in Table 2 show that all mutants maintained some amount of repair activity. Mutants C95, C95/217, and C125/217 were the most compromised, maintaining approximately 10−15% of the wild-type activity. Survival in the presence of mitomycin C corroborated the results from the UV survival assays (not shown).

Measurement of coprotease function was performed by propagating plasmid-borne *recA* mutants in a strain harboring a *recA* operator−promoter-*lacZ* fusion and observing colony color on MacConkey-lactose plates (*12*). While most mutants exhibited coprotease activity similar to that of wild-type RecA, i.e., inducible in the presence of DNA damage, or a constitutively activated coprotease function in the absence of damage, mutants C95, C95/217, and C125/217 exhibited no activity greater than the negative control (Table 2). However, these three mutant proteins showed significant in vitro LexA cleavage activity (see below).

In Vitro Activities of Mutant Proteins. To determine the ability of mutant proteins to form catalytically active oligomers in vitro, we tested each purified protein for (i) DNA binding, (ii) ATPase activity, and (iii) LexA coprotease activity.

The results of gel shift ssDNA binding assays for wild-type RecA and two mutant proteins (C217 and C121/217) are depicted in Figure 3. In the presence of ATPγS, wild-type RecA binds a significant amount of the labeled oligonucleotide, trapping a majority in the gel well, even at the lowest protein concentration that is used (0.5 μM). In the absence of ATPγS, a significant shift is not observed until the protein concentration is increased to $\approx$5 μM. As for wild-type RecA, the ssDNA binding affinity of the C217 and C121/217 mutant proteins is significantly increased by ATPγS. In the presence of ATPγS, a majority of the labeled ssDNA is shifted upward and trapped in the gel well at protein concentrations of $\geq$1.0 μM. All other mutant proteins exhibited a similar ATP dependence on ssDNA binding (data not shown). Although the ssDNA binding affinity is lowered somewhat for the mutant proteins, these results show that the allosteric response which results in an ATP-induced increase in the level of ssDNA binding is maintained in all mutants.

For wild-type RecA, we calculated a turnover number of 25.0 mol of ATP hydrolyzed min^{-1} mol of $enzyme^{-1}$ in the presence of ssDNA. Single-Cys mutant proteins C93, C95, C121, and C150 exhibited significant ATPase activity with turnover numbers varying from 12.5 to 24.5 (Table 3). In contrast, the ATPase activity of the C217 mutant and all double-Cys mutant proteins was significantly decreased, with turnover numbers varying from 2.0 to 5.5 (Table 3). These results demonstrate that the F217C mutation compromises the catalytic proficiency of ATP turnover (see below and the Discussion).

Table 3: In Vitro ssDNA-Dependent ATPase and LexA Coprotease Activities

Cys mutant	V_i/E	% LexA cleaved/60 min
93	24.5	87.0
95	17.5	84.0
121	15.8	80.0
125	nd[a]	nd
150	15.0	95.0
155	12.5	82.0
217	2.5	85.0
93/217	3.2	12.0
95/217	2.5	46.0
121/217	3.0	47.0
125/217	3.1	80.0
150/217	5.5	74.0
155/217	2.0	15.0
wild-type RecA	25.0	90.0

[a] Not determined.

All mutant proteins catalyzed the autocleavage of LexA, with activities varying from 10 to 95% cleavage/60 min (Table 3). Interestingly, several mutant proteins that exhibited a marked decrease in ATPase activity maintained a significant level of coprotease activity, e.g., C217, C95/217, C121/217, C125/217, and C150/217. This result indicates that, despite catalytic deficiencies in ATP turnover, these proteins are capable of forming a RecA−ATP−DNA complex that is activated for coprotease function.

Disulfide Cross-Linking of Mutant Proteins. Disulfide cross-linking was performed both in the absence and in the presence of DTNB to observe those cross-links which form spontaneously as well as those whose formation is assisted by thionitrobenzoate−protein mixed disulfide exchange (*20*, *21*). Following incubation in either the absence or presence of DTNB, NEM was added to prevent formation of random disulfides upon addition of SDS in preparation for gel electrophoresis. In Figure 4, we show that formation of small amounts of such random disulfides, which could otherwise interfere with the observation of intersubunit disulfides on gels, is indeed prevented by addition of NEM after the cross-linking reaction (Figure 4, compare lanes 1 and 2).

Reaction mixtures containing wild-type RecA or the single-Cys mutant protein C121, C150, C155, or C217 resulted in no bands representing higher-molecular mass cross-linked species (Figure 4). All other single-Cys mutant proteins (C93, C95, and C125) exhibited similar results (data not shown). The double-Cys mutant proteins C150/217 and C155/217 exhibited very efficient spontaneous formation of higher-molecular mass bands (Figure 5A, lanes 5 and 7). Incubation with DTNB chased nearly 100% of all monomers to higher molecular mass forms (Figure 5A, lanes 6 and 8). The double-Cys mutant protein C121/217 also exhibited both spontaneous and DTNB-induced formation of higher-molecular mass bands (Figure 5B, lanes 5 and 6), but to a lesser extent than the C150/217 and C155/217 mutants. For these three mutant proteins, a set of distinct bands is visible all the way up into the stacking gel, indicating that the cross-linking procedure has trapped various RecA filament lengths. The C93/217 and C125/217 proteins exhibited very minor amounts of higher-molecular mass bands when cross-linking was carried out in either the absence or presence of DTNB (Figure 5A,B), while the C95/217 protein exhibited the same very low level of a higher-molecular mass band only when cross-linking was carried out in the presence of DTNB

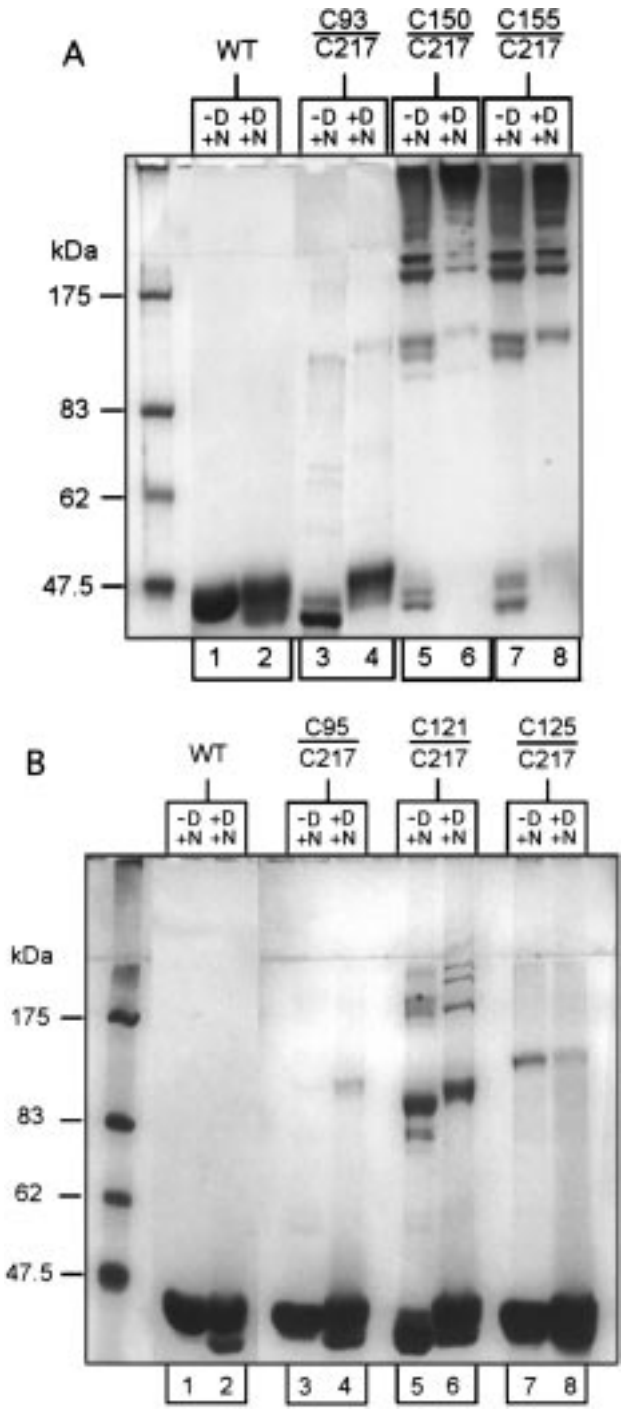

FIGURE 5: Disulfide cross-linking performed using double-Cys mutant proteins. Reaction mixtures contained 30 μM protein and were performed in the absence (−D) or presence (+D) of DTNB, followed by incubation with NEM (+N) as described in Materials and Methods. (A) Mutant proteins C93/217, C150/217, and C155/217. (B) Mutant proteins C95/217, C121/217, and C125/217.

(Figure 5B, lane 4). Low levels of cross-linked products with these three proteins were confirmed by Western blot analysis (data not shown).

Cross-linking reactions were also performed with all single- and double-Cys mutant proteins in the presence of ATP, dATP, ATPγS, ADP−AlF_4, ATPγS−ssDNA, or ADP−AlF_4−ssDNA. The results were indistinguishable from those for reactions carried out in the absence of these substrates as shown in Figures 4 and 5 (data not shown). These data suggest that the position of F217 in the RecA

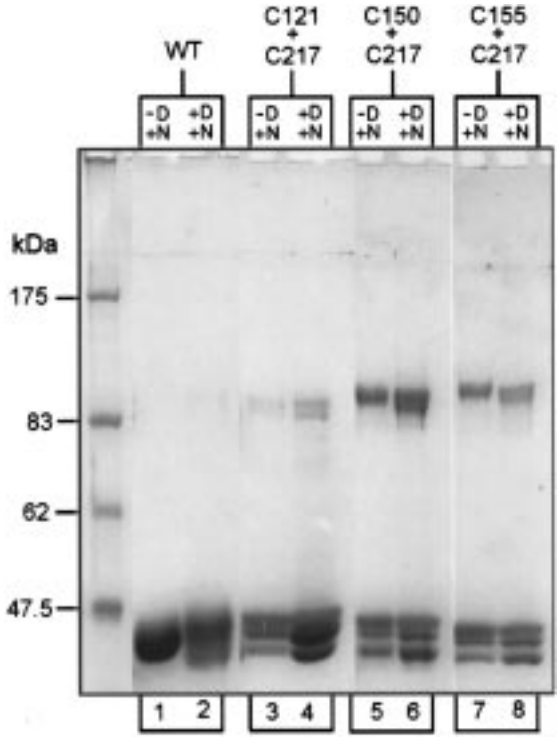

FIGURE 6: Disulfide cross-linking performed using mixtures of single-Cys mutant proteins. Reaction mixtures contained each of the indicated single-Cys mutant proteins (15 μM), and reactions were performed in the absence (−D) or presence (+D) of DTNB, followed by incubation with NEM (+N) as described in Materials and Methods.

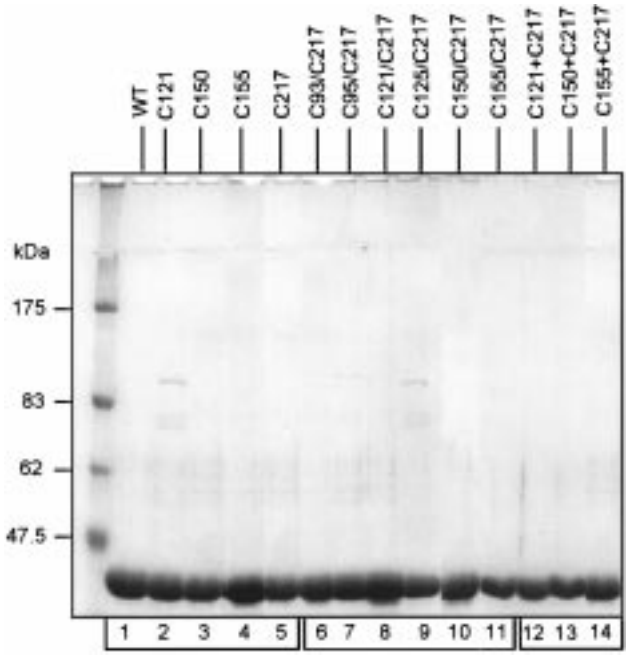

FIGURE 7: Treatment of proteins with βME following the cross-linking procedure. Reaction mixtures included the indicated proteins, and reactions were performed in the presence of DTNB followed by incubation with NEM as described in Materials and Methods. Following cross-linking, reaction mixtures were incubated with βME (150 mM) for 5 min prior to electrophoresis.

structure is the same in both the inactive and active filament forms. An alternative or additional explanation may be that cofactor-induced conformational changes which alter the positioning of residue 217 relative to amino acids in the neighboring subunit require the presence of the wild-type Phe side chain at position 217 (see the Discussion).

Cross-linking was also performed using mixes of several single-Cys mutant proteins (Figure 6). Given the fact that the RecA protein forms a head-to-tail polymeric oligomer, we expected that dimeric RecA would be the largest cross-linked species resulting from these experiments. As can be seen in Figure 6, this is the case. In either the absence or presence of DTNB, the only bands higher than monomeric RecA in mixtures of C121, C150, or C155 with C217 correspond roughly to the molecular mass of a RecA dimer (calculated value of 75.7 kDa and observed value of ≈85−90 kDa). These results demonstrate that the cross-links observed in the double-Cys mutant proteins (Figure 5) are occurring between the cross-subunit Cys mutations.

An additional set of cross-linking experiments was performed with all single- and double-Cys mutant proteins, but in this case, the reaction was followed by incubation with βME. Results depicted in Figure 7 show that in the presence of βME, all higher-molecular mass bands are resolved to a single band with a molecular mass equal to that of monomeric RecA. This demonstrates that all higher-molecular mass bands observed on the gels in Figures 5 and 6 result from the formation of disulfide bonds. Additionally, following cross-linking in either the absence or presence of DTNB, the protein bands in Figures 4−6 often appear as doublets or triplets. This is most likely due to the formation of variable amounts of intrasubunit disulfides which result in slight changes in the mobility of the protein on SDS gels. These bands are also resolved to a single band with a molecular mass equal to that of monomeric RecA following incubation with βME (Figure 7).

DISCUSSION

Within the RecA filament structure, the surface of the neighboring subunit which is close to the F217 side chain contains only minimal hydrophobic character, defined largely by I155 and the methyl group of T150 (Figure 1 and ref *7*). However, T150 can be replaced by a Ser with little effect on recombination and coprotease activities, and I155 can be substituted with a variety of residues, both polar and nonpolar, with no effect on these functions (*12*). Therefore, the requirement for a Phe residue at position 217 is not obvious from the crystal structure of RecA. A pocket can be seen in the neighboring monomer that contains several hydrophobic side chains removed from the F217 side chain by 5.4−13.6 Å ($C\beta_1-C\beta_2$ distances). The mutational stringency previously observed at position 217 (*6*) may be derived from the fact that there is a closer association between the F217 side chain and elements of this hydrophobic pocket than is apparent in the RecA crystal structure. Using a series of mutant proteins containing engineered Cys substitutions, we have examined the efficiency of disulfide formation in testing the proximity of residue 217 to positions in the neighboring monomer.

Our cross-linking procedures were designed to check for disulfide bond formation under conditions where RecA exists in either the inactive or active oligomeric form, i.e., in the absence or presence of ATPγS and ssDNA, respectively. Gel filtration profiles show that in the absence of ATPγS and ssDNA each of the mutant proteins forms high-molecular mass oligomers very similar to wild-type RecA (Figure 2).

In addition, each exhibits a significant ATPγS-induced increase in ssDNA binding affinity (Figure 3) and some level of in vivo and in vitro RecA function (Tables 2 and 3). These results demonstrate that all Cys mutant proteins in this study form both inactive filaments and catalytically active nucleoprotein complexes very similar to wild-type RecA. Therefore, the efficiency of disulfide bond formation should provide a direct measure of the cross-subunit proximity of the positions carrying the Cys substitutions in both the inactive and active oligomeric states of the protein.

The following observations indicate that the higher-molecular mass bands on cross-linking gels (Figure 5) result from cross-subunit disulfide bond formation between the designed Cys substitutions: (i) potential random disulfide bond formation being blocked by incubation with NEM immediately prior to SDS gel electrophoresis (Figure 4), (ii) the lack of similar high-molecular mass species when wild-type RecA or any of the single-Cys mutants is subjected to the same cross-linking procedure (Figure 4), (iii) cross-linking performed using mixtures of the single-Cys mutants C121 and C217, C150 and C217, and C155 and C217 showing dimeric RecA as the highest-molecular mass band (Figure 6), and (iv) all higher-molecular mass species resulting from the cross-linking procedure using any of the mutant proteins in this study being resolved to a single band of monomeric RecA by incubation with βME (Figure 7).

Cross-linking of the C217 substitution is most efficient with cross-subunit residues C150 and C155, and less efficient with C121. Although the distances between the β-carbons of position 217 and these neighboring residues are slightly larger than the "acceptable limits" for disulfides (2.9−4.6 Å) as defined by Cβ_1−Cβ_2 distances observed in protein structures and by modeling (*22*, *23*), they are clearly close enough to promote moderate (C121/217) to high levels (C150/217 and C155/217) of cross-linking. Our results are in general agreement with the position of residues in this region of the subunit interface as seen in the RecA crystal structure (see Figure 1 and Table 1). For example, we see that the cross-linking efficiency of the C121/217 protein is significantly lower than that seen with the C150/217 protein despite the fact that both T121 and T150 are equidistant from F217 (Cβ distances of 6.78 and 6.62 Å, respectively). However, this can be easily understood from the structure because the T150 side chain is oriented toward F217, while the T121 side chain points away from F217 (Figure 1).

Comparison of the cross-linking efficiencies of the C150/217 and C155/217 double mutants reveals an interesting finding that is not specifically predicted by the structure. Given the fact that T150 is more than 1 Å further from F217 than I155 is from F217 (Cβ distances of 6.62 vs 5.42 Å, respectively), we would expect to see the C155/217 mutant protein cross-link with a higher efficiency than the C150/217 protein. However, we find that the two proteins form disulfide cross-links with equal efficiencies (Figure 5). This observation is consistent with the idea that position 217 may be drawn inward toward the neighboring monomer more than is apparent in the crystal structure.

Three other double-Cys mutant proteins carry substitutions within the hydrophobic pocket at positions that are significantly further from F217 than are residues 121, 150, and 155. I93 is at the deepest part of the pocket, 13.5 Å away from F217; A125 is 10.5 Å away from F217, and A95 is 8.3 Å removed from F217 (Cβ_1−Cβ_2 distances; see Figure 1 and Table 1). Interestingly, there does appear to be a very low level of cross-subunit disulfide bond formation between C217 and these positions. Clearly, the chemistry and steric nature of the wild-type Phe versus the mutant Cys side chains are different, and the Cys substitution may significantly diminish the extent of or preclude an ATP-induced entry of this residue into the hydrophobic pocket in the neighboring monomer. The fact that we see no difference in the efficiency of disulfide bond formation whether cross-linking is carried out in the absence or presence of ATPγS and ssDNA supports this idea. However, these results also suggest that position 217 can, in fact, be closer to positions 93, 95, and 125 than is apparent in the RecA crystal structure.

While our cross-linking studies are in general agreement with the position of the F217 side chain within this region of the subunit interface as seen in the crystal structure, our functional studies suggest that ATP-induced movement of F217 plays a role in mediating structural changes that are important in establishing an enzyme conformation that is competent for ATP turnover. Analysis of both in vivo and in vitro RecA functions shows that all mutants which carry the F217C substitution are far more proficient for activities that require only ATP binding (ATP-induced increase in DNA binding affinity, in vivo coprotease activity, and the extent of in vitro LexA cleavage) as opposed to activities that require ATP turnover (recombinational DNA repair and ssDNA-dependent ATP hydrolysis). These data suggest that F217 is involved in mediating ATP-induced conformational changes that result in optimal positioning of residues that are involved in nucleotide hydrolysis, and that these changes are largely independent of those required for ATP-mediated high-affinity DNA binding. Glu96 has been proposed to serve as the general base that activates water for an in-line attack on the γ-phosphate of ATP, and Asp144 is involved in positioning the active site Mg^{2+} (*24*). We note that these residues in the ATP catalytic site are very close to the region of the subunit interface containing F217 (Figure 1).

We also find that while all mutant proteins carrying the C217 mutation form high-molecular mass filaments similar to wild-type RecA, they no longer exhibit an ATP-induced shift in their oligomeric distribution (Figure 2). Although we do not understand how this particular ATP-mediated effect relates to RecA function or to other ATP-induced conformational changes in protein structure, we are currently investigating this issue.

A number of ATP-induced conformational transitions have been observed for RecA. (i) ATP binding promotes a transition to a high-affinity DNA binding form (*25*−*27*), a transition mediated in large part by Gln194 within the ATP binding site (*24*, *28*). (ii) Limited proteolysis studies revealed a NTP-induced conformational change in or near the L1 region, residues 156−165 (*29*). (iii) Various techniques, including electron microscopy, light scattering, and gel filtration (*8*, *17*−*19*), have demonstrated an ATP-induced change in the oligomeric distribution of RecA. (iv) Electron microscopic studies have revealed a significant ATP- and DNA-induced increase in the helical pitch of the RecA filament (*9*), an effect which undoubtedly involves reorganization of various regions of the subunit interface. Data from this study suggest that the region of the subunit interface surrounding F217 contains important determinants of ATP-

induced allosteric changes in the RecA structure, and that F217 is a critical player in these events. Specifically, we propose that F217 is important for the proper orientation of catalytic residues within the ATP binding site of the neighboring subunit, and that the required conformational changes result from an ATP-induced movement of the F217 side chain relative to positions within a hydrophobic pocket in the neighboring subunit as defined in Figure 1. Ongoing work is designed to provide further mechanistic detail regarding allosteric transitions mediated by F217, and to identify other residues in this area which play a role in these effects.

ACKNOWLEDGMENT

We are grateful to members of the Knight lab, and especially to Dr. William Royer, for comments on the manuscript.

REFERENCES

1. Radding, C. M. (1989) *Biochim. Biophys. Acta 1008*, 131−145.
2. Roca, A. I., and Cox, M. M. (1990) *Crit. Rev. Biochem. Mol. Biol. 25*, 415−456.
3. Little, J. W. (1991) *Biochimie 73*, 411−422.
4. Kowalczykowski, S. C., Dixon, D. A., Eggleston, A. K., Lauder, S. D., and Rehrauer, W. M. (1994) *Microbiol. Rev. 58*, 401−465.
5. Cox, M. M. (1999) *Prog. Nucleic Acid Res. Mol. Biol. 63* (in press).
6. Skiba, M. C., and Knight, K. L. (1994) *J. Biol. Chem. 269*, 3823−3828.
7. Story, R. M., Weber, I. T., and Steitz, T. A. (1992) *Nature 355*, 318−325.
8. Logan, K. M., Skiba, M. C., Eldin, S., and Knight, K. L. (1997) *J. Mol. Biol. 266*, 306−316.
9. Egelman, E. H. (1993) *Curr. Opin. Struct. Biol. 3*, 189−197.
10. Sambrook, J., Fritsch, E. F., and Maniatis, T. (1989) *Molecular Cloning: A Handbook*, 2nd ed., Cold Spring Harbor Laboratory Press, Cold Spring Harbor, NY.
11. Logan, K. M., and Knight, K. L. (1993) *J. Mol. Biol. 232*, 1048−1059.
12. Nastri, H. G., and Knight, K. L. (1994) *J. Biol. Chem. 269*, 26311−26322.
13. Konola, J. T., Nastri, H. G., Logan, K. M., and Knight, K. L. (1995) *J. Biol. Chem. 270*, 8411−8419.
14. Weinstock, G. M., McEntee, K., and Lehman, I. R. (1981) *J. Biol. Chem. 256*, 8845−8849.
15. Kowalczykowski, S. C., and Krupp, R. A. (1995) *Proc. Natl. Acad. Sci. U.S.A. 92*, 3478−3482.
16. Weisemann, J. M., and Weinstock, G. M. (1988) *DNA 7*, 389−398.
17. Brenner, S. L., Zlotnik, A., and Griffith, J. D. (1988) *J. Mol. Biol. 204*, 959−972.
18. Heuser, J., and Griffith, J. (1989) *J. Mol. Biol. 210*, 473−484.
19. Wilson, D. H., and Benight, A. S. (1990) *J. Biol. Chem. 265*, 7351−7359.
20. Sauer, R. T., Hehir, K., Stearman, R. S., Weiss, M. A., Jeitler-Nilsson, A., Suchanek, E. G., and Pabo, C. O. (1986) *Biochemistry 25*, 5992−5998.
21. Creighton, T. E. (1993) in *Proteins: Structures and Molecular Properties*, pp 19−20, W. H. Freeman and Co., New York.
22. Hazes, B., and Dijkstra, B. W. (1988) *Protein Eng. 2*, 119−125.
23. Sowdhamini, R., Srinivasan, N., Shoichet, B., Santi, D. V., Ramakrishnan, C., and Balaram, P. (1989) *Protein Eng. 3*, 95−103.
24. Story, R. M., and Steitz, T. A. (1992) *Nature 355*, 374−376.
25. Silver, M. S., and Fersht, A. R. (1982) *Biochemistry 21*, 6066−6072.
26. Menetski, J. P., and Kowalczykowski, S. C. (1985) *J. Mol. Biol. 181*, 281−295.
27. Menetski, J. P., and Kowalczykowski, S. C. (1988) *Biochemistry 27*, 1205−1212.
28. Kelley, J. A., and Knight, K. L. (1997) *J. Biol. Chem. 272*, 25778−25782.
29. Kobayashi, N., Knight, K. L., and McEntee, K. (1987) *Biochemistry 26*, 6801−6810.

BI991118Z